Photochemical & Photobiological Sciences

COMMUNICATION

Title

Response of sweet pepper autofluorescence against solar radiation

Authors information

Tetsuyuki Takemoto[1,2]†, Keiji Konagaya[3]†*, Makoto Kuramoto[4], Satoru Fukugaichi[5,3], Naoshi Kondo[2]

†These authors contributed equally as co-first authors.

* Corresponding author: Keiji Konagaya (konakei@icloud.com)

1 Kyoto Prefectural Agriculture, Forestry and Fisheries Technology Center, Kameoka 621-0806, Japan

2 Graduate School of Agriculture, Kyoto University, Kyoto 606-8502, Japan

3 Faculty of Collaborative Regional Innovation, Ehime University, Matsuyama 790-8577, Japan

4 Advanced Research Support Center (ADRES), Ehime University, Matsuyama 790-8577, Japan

5 Paper Industry Innovation Center, Ehime University (PIICE), Matsuyama 790-8577, Japan

Keywords

Sweet pepper (*Capsicum annuum* L.), Sunlight exposure, Blue autofluorescence, Epidermal development

Statements and declarations

There are no conflicts to declare.

1. Introduction

Sweet pepper (*Capsicum annuum* L.) is a major horticultural crop rich in vitamin C [1] and is attracting increasing attention owing to its health benefits. However, although its yield and quality per area have improved in recent decades due to technical advances, pests and diseases still cause yield declines [2]. Even though pesticides partially prevent diseases, their inappropriate use harms the ecosystem and human health. Moreover, yield loss occurs due to poor growth during the pre-harvest phase [3]. Therefore, in horticulture, maintaining a suitable environment is important to realise integrated pest management (IPM) and improve the quality and yield of the crops.

One of the causes of poor crop growth is the damage caused by high-level sunlight exposure (including high temperature and dryness caused by the exposure) [2]. In extreme cases, it also causes sunburns, damaging plants' epidermis [4] . Therefore, shading technology has been developed and is being used in greenhouses to prevent these issues [5] . As a result, on average, the amount of sunlight exposure could be reduced by shading; however, it is difficult to determine the optimum shading for each plant (each fruit) as it is impossible to predict each biological response to sun exposure. Nevertheless, we can adjust the shading and other environmental factors (irrigation, temperature and soil fertility) more precisely if we know the responses of sweet pepper to sunlight exposure. This information could enhance the yield and quality of the product [2] .

Pyranometers [6] and photosensitive films [7] have been used to determine the amount of solar radiation in greenhouses. However, these methods alone have not determined crop responses to solar radiation. Moreover, to the best of our knowledge, there are no means or practical techniques in horticulture to fully understand plant’s responses to sunlight exposure. Moreover,

large variations in autofluorescence (blue emission observed non-destructively) have been previously reported among fruits of the *Capsicum* genus [8] . Therefore, the authors utilised an intense light emitting diode (LED) semiconductor as the excitation (365 nm) source in a previous study. The observations showed an accumulation of UV-absorbing compounds (including UV-excited fluorophores) and another 'colour' (fluorescence) that appeared when fruits were illuminated under the 365 nm UV light. According to photochemistry and photobiology, this fluorescence variation can be due to a variation in the amount of UV-absorbing compounds [9 – 1 1] and UV-excited fluorophores among the fruits [1 2] . The variations in these compounds should be determined in the growing phase of the sweet peppers before the observation. If this hypothesis is true, we could potentially determine the response of sweet pepper to solar radiation non-destructively by only observing the surface autofluorescence.

Based on these facts, in this study, we hypothesised that sunlight affects the sweet peppers' 365 nm excited-blue autofluorescence. To examine this, we investigated the autofluorescence images of the fruits grown under sunlit (normal) and shaded (half-normal) conditions. Finally, we proposed a potential application of this blue autofluorescence.

2. Results

To investigate the effect of the solar radiation level on sweet pepper blue autofluorescence, fluorescence images of fruits grown under different radiation levels were obtained. Two conditions were set: shaded (approximately half of the normal) and sunlit (normal) greenhouses, by changing the extent of shading (Fig. S1).

Although bright-blue fluorescence was observed on the surface of the fruits grown under shaded conditions, two patterns of fluorescent fruits—bright and dark—were observed under the sunlit condition (Fig. 1a). Therefore, to confirm these trends quantitatively, the fluorescence spectrum of the fruits was observed using a fluorophotometer after excitation at 360 nm (which is close to the

fluorescence images at 365 nm) (Fig. 1b). In both shaded and sunlit conditions, the spectra exhibit two features: blue and red emission with a peak at 390 nm and 700 nm, respectively. The observations were in accordance with the reddish-blue and purple colours observed in the autofluorescence images (Fig. 1a) (as in the experimental section, fluorescence at ~550 nm and > 695 nm was excluded). Subsequently, to explore the blue emission in detail, the fluorescence intensity at 390 nm, which is the edge of the spectral range, was further analysed (Fig. 1c). Under shaded conditions, the fluorescence intensity varied from 550 a.u. to 1000 a.u., while in sunlit conditions, it varied from a lower value of approximately 200 a.u. to 1000 a.u. Besides, the mean values were statistically different, as obtained by t-test ($P < 0.05$). Investigations also revealed that the shoulder peak at 450 nm was similarly attenuated during the sunlit condition. Thus, the minimum fluorescence intensity value under the normal exposure condition was no more than half of that under the shaded condition. The red emission range also observed a decrease in the fluorescence intensity under sunlit conditions. Since 2nd order diffraction light of 360 nm ($\sim 2\lambda_{ex}$ = 720 nm) was removed in the red emission range (Fig. 1b), we alternatively analysed the red emission spectra excited at 460 nm (a typical wavelength of chlorophyll excitation for green peppers [8] and kiwi fruit [1 3]). The red emission (695 nm) was lower for fruits grown under sunlit conditions (Fig. S2), and statistical significance was at $P < 0.05$, as obtained by the t-test. The red emission excited by UV light can be ascribed to chlorophyll, considering that it is observed over a wide range of excitation wavelengths and its large Stokes shift. Therefore, we can infer that the red emission decreased for sunlit samples when excited at 365 nm as well. Hence, we discovered that the dark fluorescence of the sweet pepper fruit only appeared in sunlit growing conditions: The ‘dark’ is defined as the weak observation of blue fluorescence by the naked eye under 5-mW cm^{-2} illumination at 365 nm.

The fluorescence results validated our hypothesis that sunlight exposure affects the autofluorescence of the sweet pepper fruits (0.7-fold decline at emission of 390 nm for low exposure conditions). However, a biological understanding of the phenomenon is necessary to use

this autofluorescence phenomenon. Hence, we investigated the tissues that emit blue autofluorescence to determine their physiological background. Fluorescence microscopic images of the pericarp, obtained from the cross-sectional region, were taken at the same excitation wavelength (365 nm) as that of the autofluorescence images (Fig. 2). As a result, tissues near the surface emitted blue autofluorescence (within 50 μm in the depth direction), while inner tissues emitted red fluorescence. Although the outermost region also slightly emitted red fluorescence (Fig. 2), this emission came from the back of the depth of focus; thus, the genuine outermost layer of the sweet pepper fruit emitted blue autofluorescence. The microtome-sectioned specimen also emitted blue fluorescence in the outermost cell layer (Fig. S3). In this sample, the cytosol was washed out of the glass slide in an experimental step. These results suggest that the blue emission came from the epidermal cell layers, as the emission occurred within 50 μm of the surface. From this we can infer that the sweet pepper autofluorescence response occurred within the epidermal scale as the excitation and emission light penetrated and propagated within this scale.

To further investigate the anatomical changes in the epidermal tissue, microtome sections of fruit samples with different exposure levels were observed under a microscope. The cuticle of the epidermis appeared thicker for the samples in sunlit conditions with Oil Red O (ORO) staining (Fig. 3a). The cuticle has two structural features: the outer flat part and the invagination part between the epidermal cells. We observed that the former structure was thicker in cuticles from the sunlit samples. On average, it was also observed that the epidermal wall thickness was approximately 4 μm wider (1.3-fold thicker) in the sunlit samples compared to that in the shaded samples (Fig. 3b), as observed previously [9] . Besides, the average values for the two conditions were significantly different, as obtained by t-test ($P < 0.05$). Therefore, considering these results, the following can be inferred: sunlight exposure promoted epidermal development and altered blue emission of sweet pepper fruits.

UV-absorbing pigments play a important role in protecting plant tissues from UV radiation [9 – 11] ; thus, their UV absorption properties could explain the correlation between epidermal

development and blue-light autofluorescence. Therefore, the diffuse transmittance of the isolated epidermal cell wall (Fig. 4a) was investigated in the UV-Vis range (250–700 nm). Two absorption bands were observed below 250 nm and 300 nm (Fig. 4b). Since the 300 nm peak is closely related to the blue fluorescence excited by UVA (365 nm), we further analysed the absorbance at 300 nm (Fig. 4c). The absorbance of the epidermal cell wall was significantly higher in the sunlit condition than in the shaded condition (1.2-factor increase; $P < 0.1$, as obtained by t-test). This result strongly suggests that the excitation light and blue emission were highly attenuated by the accumulation of UVB-absorbing pigments, as previously reported in sunflower leaves [1 1] .

In this study, we found that sweet pepper fruits with dark blue autofluorescence always grew in sunlit conditions. However, the fluorescence intensity and amount of solar radiation did not exhibit a direct relationship. For example, the maximum fluorescence intensity distribution did not change depending on the sunlight conditions (Fig. 1c). One reason for this could be that in a greenhouse with a large amount of sunlight exposure, even if the frequency of leaf hiding is the same as that of the other conditions, the variation in the absolute value of solar radiation is large. In contrast to the same maximal fluorescence intensity levels, the maximum thickness and UV absorbance values differed at different solar radiation levels (Fig. 3b, Fig. 4c). Therefore, autofluorescence alone is neither enough to predict thickness and UV absorbance in the epidermis nor the crop yield. Assuming that the scattering effect within the epidermal cell wall is relatively small (at the scale of 10 μm), the underlying mechanism can be further understood by investigating the two groups of UV-absorbing pigments: strongly fluorescent pigment(s) (contributing to the emission) and other(s) (contributing to the extinction).

3. Conclusions

In this study, we examined the hypothesis that the level of sunlight exposure of sweet peppers during growth affects the blue autofluorescence under 365 nm illumination. To test this hypothesis, we cultivated sweet peppers in a greenhouse with high (normal) and low (half of the normal)

157 sunlight exposure levels. Consequently, dark-fluorescent fruits appeared only under sunlit
158 conditions. By observing and spectroscopically characterising the epidermis and cuticle, we also
159 found the accumulation of UVB-absorbing pigments (~300 nm of the peak) and concomitant
160 epidermal development in samples under high sunlight exposure conditions. This study also
161 showed that the blue autofluorescence under sunlit conditions varies greatly. This reflects the
162 non-uniformity of sunlight levels, even within a greenhouse. Sweet pepper blue autofluorescence
163 has the potential to determine the response against the solar radiation at the fruit level, which cannot
164 be achieved using other methodologies.
165
166 **4. Experimental procedure**
167 ***4.1 Fruit material***
168 Sweet pepper (*Capsicum annuum* L.) plants (cultivar 'Kyoto Manganji No. 2') were cultivated
169 in a greenhouse in Kyoto Prefectural Agriculture, Forestry and Fisheries Technology Center
170 (Kameoka, Kyoto). The greenhouse was 7.2 m wide and 20 m long, and 3.3 m and 1.7 m high at
171 the center and the side pole, respectively. Pruned tree-based compost of 3000 kg $10a^{-1}$ and 180-day
172 sigmoid type polyolefin-coated fertilizer (NPK 14:11:13 %) of 214 kg $10a^{-1}$ were applied as basal
173 dose during field preparation. Irrigation was done when necessary with automatic irrigation system
174 based on the value of soil moisture. Seedlings were transplanted on 5 April 2021. From the fruit set
175 to the harvest, the maximum air temperatures were 37.7°C and 37.4°C for the shaded and the sunlit
176 areas, respectively. The average values were 26.3°C and 26.3°C, and and the minimum values
177 were 17.5°C and 18.2°C for the shaded and the sunlit conditions, respectively. These data
178 demonstrated the solar radiation conditions did not affect the air temperatures in our conditions.
179 The polyolefin shading material, comprising a coating 5 + 1 (C.I. TAKIRON Corporation,
180 Japan), with 0.1 mm thickness, was used to cover the greenhouse during the sampling period (Fig.
181 S1a, d). Integrated solar radiations (MJ m^{-2}), from two weeks before harvesting (usual fruits
182 elongating period) of each treatment, were converted from solar radiations (kW m^{-2}) that were

183 measured using the pyranometer PVSS-01 (SANKO Co., LTD. Japan), which was positioned at
184 1.8 m above the ground level. The instruments have a spectral response from 400 to 700 nm.
185 Integrated solar radiations of shaded and sunlit areas were 113 MJ m^{-2} and 178 MJ m^{-2},
186 respectively. By converting the coefficient for daylight (4.57 μmol J^{-1}) [14], the integrated
187 photon flux density for the period after fruit set to harvest was estimated to be 510 mol m^{-2} and 810
188 mol m^{-2} for the shaded and sunlit areas, respectively.
189 On the day of the harvest, 104 fruits, stored at 10–15 °C, were sent via commercial delivery to
190 Ehime University and were received the next day. Then, they were stored in a cooling incubator
191 (IN604, Yamato Scientific Co., Ltd., Japan) at 8–13 °C and 80–90% relative humidity until further
192 analysis. As the autofluorescence on the surface did not change for 1 week, the experiment was
193 completed within 1 week of the arrival of the samples. To minimise the evaporation of water
194 during storage, the entire sample for each condition was covered with kitchen wrap. For each
195 growth condition, 20 fruits of a standard size without any defects were selected (40 fruits in total).
196 To confirm that the fruit developmental stage was similar, fruit length was measured with a calliper
197 (Fig. S4). A series of independent experiments were performed twice using the selected samples.
198
199 ***4.2 Transmission properties of the shading-material***
200 Diffuse transmission spectrum was measured to determine the transmittance of the
201 light-shielding material for each wavelength using a UV/Vis/near-infrared spectrophotometer
202 (SolidSpec-3700, Shimadzu Corporation, Japan) and an integrating sphere unit. According to the
203 manual, the wavelength range was set to 250–700 nm, while the wavelength interval and the
204 bandwidth were set at 0.5 nm and 8 nm, respectively. A single-beam mode was used, and the
205 baseline and dark signals were recorded before and after the experiment, to confirm the stability.
206 The repetitive unit size of the shading material was of the order of centimetres, which is not
207 negligible compared to the window size of 12 mm (horizontal) × 20 mm (vertical); thus, the diffuse
208 transmittance for each part of the material was multiplied by the area fraction. Consequently, the

effective transmittance for each growth condition was calculated by multiplying the number of sheets stacked in the field (Fig. S1a):

$$T_{\mathrm{eff}} = \Sigma\, T_{\mathrm{i}} f_{\mathrm{i}} \quad \text{Eq. (1),}$$

where T_{eff} is the effective transmittance of each shading material, T_{i} is the transmittance of each part of the material, and f_{i} is the area fraction of that part of the material. The transmittances of both the materials used under shaded and sunlit conditions were measured at two points (a thick and a thin part in Fig. S1b). The effective transmittance under shaded conditions was approximately half of that under sunlit conditions (Fig. S1c).

4.3 Autofluorescence imaging

To photograph the autofluorescence of the sweet pepper fruit, we used the same setup as previously reported [8] . A 365 nm light source (LDR2-60UV2-365-N, CCS Inc., Japan) was placed at a height of 25 cm above the table to ensure irradiation of the sample surface in the range of 0.5–5.0 mW cm^{-2}. The UV irradiance was measured using a UV meter (UVA-365, Custom Inc., Japan; centre wavelength, 355 nm; half-width of sensitivity, 330–370 nm). This exposure level (150 J m^{-2} for 3 s) is at least three orders of magnitude lower than that during the growing stage (typically MJ m^{-2} after fruit set). No photobleaching was observed within the time range of 1–3 s. A digital camera (Canon EOS Kiss X7, Canon Inc., Japan) was fixed on the ring-type UV LED with a jig to acquire the images. The focal length was set to 20–30 mm by changing the magnification such that focus was on the sample fruit. The shutter speed was set at 1/20 s to prevent blurring. The F-value and ISO were set to 5.6 and 1600, respectively. A long-pass filter (FGL400S, Thorlabs Japan Inc., Japan) with a cut-on wavelength of 400 nm was attached to the front of the lens to eliminate reflection of the excitation light. For reference, colour images were captured under the

illumination of a fluorescent lamp. For the colour image, the shutter speed and the white balance were set at 1/30 s and 4000 K, respectively.

4.4 Fluorescence spectra

To quantify the autofluorescence of sweet pepper excited at 360 nm, the same samples used for photography were used for the spectral measurements. A pericarp disc of 20 mm diameter was created with a punch near the equator of the fruit. It was then placed into a quartz cell and the fluorescence emission from the outer surface was recorded (the signal was comparable to that observed non-destructively [8]). Samples were obtained from two locations on opposite sides of the fruit surface, and the average value was calculated for that fruit. Fluorescence intensity was measured using a fluorometer (RF-6000, Shimadzu Corporation, Japan). The excitation wavelength was set at 360 nm, and the emission range was set from 390 nm to 750 nm with 1 nm intervals. The scan speed was 6000 nm min^{-1}, and the bandwidth was 5 nm for both the slits. Moreover, since Raman emission was observed near 550 nm in the preliminary experiment (Fig. S5), this range was excluded. In addition, to eliminate the 2nd order diffraction of the excitation light ($2\lambda_{ex}$ = 740 nm), this range was also excluded. Consequently, chlorophyll fluorescence at approximately 690 nm and 740 nm could not be observed; hence, other excitation spectra at 460 nm were collected. The measured emission range was 490–750 nm. The incident angle of the excitation light and the detection angle of the fluorescence were both 45°. The stability of the detector was confirmed daily during the experiment using the Raman band of water excited at 350 nm.

4.5 Autofluorescence microscopy imaging of hand-sectioned samples

Microscopic images of the autofluorescence were captured to determine the tissues that emitted blue fluorescence. One fruit sample of a standard length was selected for each exposure condition. Subsequently, a 1 cm-wide ring-shaped sample was sliced parallel to the cross-section by using a

razor. Imaging was performed within 5 min of sample cutting and illumination was minimised to prevent photobleaching (approximately, 8–15 mW cm^{-2}, i.e. 450 J m^{-2} for 3 s). This UV dose was at least three orders of magnitude lower than that used during the growth (MJ m^{-2} from fruit set to harvest). No fluorescence photobleaching was observed when the observation duration was changed from 1 s to 3 s. A high-power LED (Omnicure LX405S, Lumen Dynamics Group Inc., Canada) with a central wavelength of 365 nm was used as the excitation source. LED output position was fixed at approximately 4 cm from the sample surface with an elevation angle of 45°. This distance ensured sufficient luminous intensity of the emission and sample space when using a lens (focal length of 12 mm). A 3R-MSTVUSB273 microscope (3R SYSTEMS CORP., Japan) was used for the observation, and a 5-million-pixel CMOS (optical zoom 4×) was used as the image sensor. A long-pass filter, FGL400S (Thorlabs Japan Inc., Japan), was attached to the front of the lens to remove the reflected light (same as that used for whole fruit photography).

4.6 Isolation of epidermal cell wall

To investigate the thickness of the epidermal cell wall (e.g. approximation of the cuticle) and its light transmission, the epidermal cell wall was enzymatically isolated as reported previously [8] . Since the cell wall on the outside of the epidermis is synonymous with the cuticle, the thickness of this sample can be considered as an approximation of the thickness of the cuticle. A 30 mm diameter pericarp disc was dipped in an enzyme cocktail containing 4.0% w/v pectinase and 0.4% w/v cellulase in 50 mM sodium citrate buffer (pH 4.0) with 1 mM sodium azide [1 5 , 1 6] . Samples were incubated with PIC100 (AS ONE Corporation, Japan) at 35 °C for 3–4 days to isolate the cell wall outside the epidermis. The cell wall was then air-dried at 35 °C overnight and stored in a dry place until further analysis. Removal of the cellular structures was confirmed by preliminary experiments using microscopy and ORO staining. This sample was referred to as the ‘dry’ epidermal cell wall to distinguish it from the ‘intact’ epidermal cell wall.

4.7 Staining of microtome-sectioned cuticle samples

To examine the development of the cuticle under the same solar conditions in the same samples, microtome sections of frozen pericarps were stained with ORO stain and observed under a microscope [1 7] . At the equator of the fruit, a 5 × 5 mm^2 square sample was immersed in FFA fixative (95% ethanol, distilled water, 35% formaldehyde, and glacial acetic acid in a 50:35:10:5 ratio) for 1–3 days and dissolved in phosphate buffered saline. They were then cryoprotected with 10% sucrose. The samples were embedded in OCT compound (Sakura Finetek Japan Co., Ltd., Japan), frozen in isopentane (FUJIFILM Wako Pure Chemical Corporation, Japan), cooled in liquid nitrogen, and stored at −30 °C until sectioning. Then, the pericarp was sectioned into 5−8 μm thickness using a cryomicrotome (CM1860 UV, Leica Microsystems, Germany) at −20 °C. Cross-sectional or longitudinal sections were cut and post-fixed with FFA, washed with distilled water, and dried. The sections were then stained with 60% ORO stain for 30 min, washed with 50% isopropanol and distilled water, and dried. The imaging was performed in a bright field using an optical microscope (TS100-F, Nikon Corporation, Japan) with an objective lens of 4× (NA, 0.13; WD, 16.5 mm). More than 20 images of different fields of view were captured for each solar condition. Additionally, to correlate with the cuticle development, the thickness of the dried epidermal cell wall was measured using a micrometer MDQ-30 (Mitutoyo Corporation, Japan). For each fruit, samples were obtained from two locations in opposite directions at the equator, and three locations were measured per sample with a minimum reading unit of 1 μm.

4.8 Autofluorescence microscopy imaging of microtome-sectioned samples

To verify the tissue emitting the blue autofluorescence near the epidermis, unstained cuticle microtome sections were observed by fluorescence microscopy (BX-3500TFL, WRAYMER INC., Japan) with an attached 4× (dry NA, 0.1; WD, 17.9 mm) objective lens with an irradiance at the focal point of 0.8 mW mm^{-2}. The illumination of the excitation light was minimised to prevent photobleaching. This irradiance was at least three orders of magnitude lower than the level of the

cumulative amount of solar radiation (MJ m^{-2}) during the growth process, even when it was assumed that irradiation duration was 2 s (i.e. 1.6 kJ m^{-2}). No fluorescence breach was observed when the exposure time was varied from 1 s to 2 s. An LED and mercury lamps (20 V, 5.5 A) were used for bright-field and fluorescence analyses, respectively. An excitation filter with a half-width of 320–370 nm and a centre of 350 nm, long-pass filter with a cut-on wavelength of 430 nm, and a dichroic mirror were used for these analyses.

4.9 Transmission spectra of the epidermal cell wall

To investigate the accumulation of UV-absorbing compounds in the epidermal cell wall, the diffuse transmission spectra of the dried samples were measured. The transmittance was measured in the same manner as that of the light-shielding material. However, the samples were carefully treated to prevent breakage. Absorbance is shown in $\log_{10}(1/T)$ (where T is the transmittance), which correlates with the accumulation of UV-absorbing compounds.

Acknowledgements

We greatly appreciate Prof. Koji Omori (Faculty of Collaborative Regional Innovation, Ehime University, Japan) for providing the experimental tools. We also thank Mr. Koki Kida for his support with our experiments. Other parts of the experiment were also conducted with the aid of the Advanced Research Support Center, Ehime University. This work is supported in part by Adaptable and Seamless Technology transfer Program through Target-driven R&D (A-STEP) from Japan Science and Technology Agency (JST) Grant Number JPMJTM20PQ.

Author contributions

All the authors contributed to the conception and design of the study. Material preparation, data collection, and analysis were performed by Tetsuyuki Takemoto and Keiji Konagaya. The first

draft of the manuscript was written by Keiji Konagaya and Tetsuyuki Takemoto, and all the authors commented on the previous versions of the manuscript. All the authors have read and approved the final manuscript.

References

1. Frank, C. A., Nelson, R. G., Simonne, E. H., Behe, B. K., & Simonne, A. H. (2001). Consumer preferences for color, price, and vitamin C content of bell peppers. *HortScience*, *36*(4), 795–800. https://doi.org/10.21273/HORTSCI.36.4.795
2. Bosland, P. W., Votava, E. J., & Votava, E. M. (2012). *Peppers: Vegetable and spice capsicums*. CABI.
3. FAO. (2011). *Global food losses and food waste–Extent, causes and prevention*. https://www.fao.org/3/i2697e/i2697e.pdf
4. Munné-Bosch, S., & Vincent, C. (2019). Physiological Mechanisms Underlying Fruit Sunburn. *Critical Reviews in Plant Sciences*, *38*(2), 140–157. https://doi.org/10.1080/07352689.2019.1613320
5. Fukuda, N. (2013). Advanced light control technologies in protected horticulture: A review of morphological and physiological responses in plants to light quality and its application. *Journal of Developments in Sustainable Agriculture*, *8*(1), 32–40. https://doi.org/10.11178/jdsa.8.32
6. Zhang, Q. (2015). *Precision Agriculture Technology for*

Crop Farming. CRC Press.

7. Kumagai, E. (2018). Effect of early sowing on growth and yield of determinate and indeterminate soybean (*Glycine max* (L.) Merr.) cultivars in a cool region of northern Japan. *Journal of Agricultural Meteorology*, *74*(1), 18–28. https://doi.org/10.2480/agrmet.D-17-00009

8. Konagaya, K., Omwange, K. A., Al Riza, D. F., Khaliduzzaman, A., Martínez Oliver, A., Rovira-Más, F., Nagasato, H., Ninomiya, K., & Kondo, N. (2020). Association of fruit, pericarp, and epidermis traits with surface autofluorescence in green peppers. *Photochemical & Photobiological Sciences*, *19*(12), 1630–1635. https://doi.org/10.1039/D0PP00236D

9. Trošt Sedej, T., Erznožnik, T., & Rovtar, J. (2020). Effect of UV radiation and altitude characteristics on the functional traits and leaf optical properties in *Saxifraga hostii* at the alpine and montane sites in the Slovenian Alps. *Photochemical & Photobiological Sciences*, *19*(2), 180–192. https://doi.org/10.1039/C9PP00032A

10. Solovchenko, A., & Merzlyak, M. (2003). Optical properties and contribution of cuticle to UV protection in plants: Experiments with apple fruit. *Photochemical & Photobiological Sciences*, *2*(8), 861. https://doi.org/10.1039/b302478d

11. Stelzner, J., Roemhild, R., Garibay-Hernández, A., Harbaum-Piayda, B., Mock, H.-P., & Bilger, W. (2019).

391 Hydroxycinnamic acids in sunflower leaves serve as
392 UV-A screening pigments. *Photochemical &*
393 *Photobiological Sciences*, *18*(7), 1649–1659.
394 https://doi.org/10.1039/C8PP00440D
395 12. Lakowicz, J. R. (2013). *Principles of fluorescence*
396 *spectroscopy*. Springer Science & Business Media.
397 13. Novo, J. M., Iriel, A., & Lagorio, M. G. (2012).
398 Modelling chlorophyll fluorescence of kiwi fruit
399 (Actinidia deliciosa). *Photochemical & Photobiological*
400 *Sciences*, *11*(4), 724.
401 https://doi.org/10.1039/c2pp05299g
402 14. Thimijan, R. W., & Heins, R. D. (1983). Photometric,
403 Radiometric, and Quantum Light Units of Measure A
404 Review of Procedures for Interconversion. *HortScience*,
405 *18*(6), 818–822.
406 15. Li, Y., Li, Q., & Chen, B. (2016). Organic pollutant
407 penetration through fruit polyester skin: A modified
408 three-compartment diffusion model. *Scientific Reports*,
409 *6*(1), 23554. https://doi.org/10.1038/srep23554
410 16. Shafer, W. E., & Bukovac, M. J. (1987). Effect of acid
411 treatment of plant cuticles on sorption of selected
412 auxins. *Plant Physiology*, *83*(3), 652–656.
413 https://doi.org/10.1104/pp.83.3.652
414 17. Isaacson, T., Kosma, D. K., Matas, A. J., Buda, G. J., He,
415 Y., Yu, B., Pravitasari, A., Batteas, J. D., Stark, R. E.,
416 Jenks, M. A., & Rose, J. K. C. (2009). Cutin deficiency

417 in the tomato fruit cuticle consistently affects
418 resistance to microbial infection and biomechanical
419 properties, but not transpirational water loss. *The Plant*
420 *Journal*, *60*(2), 363–377.
421 https://doi.org/10.1111/j.1365-313X.2009.03969.x
422

Figure Captions

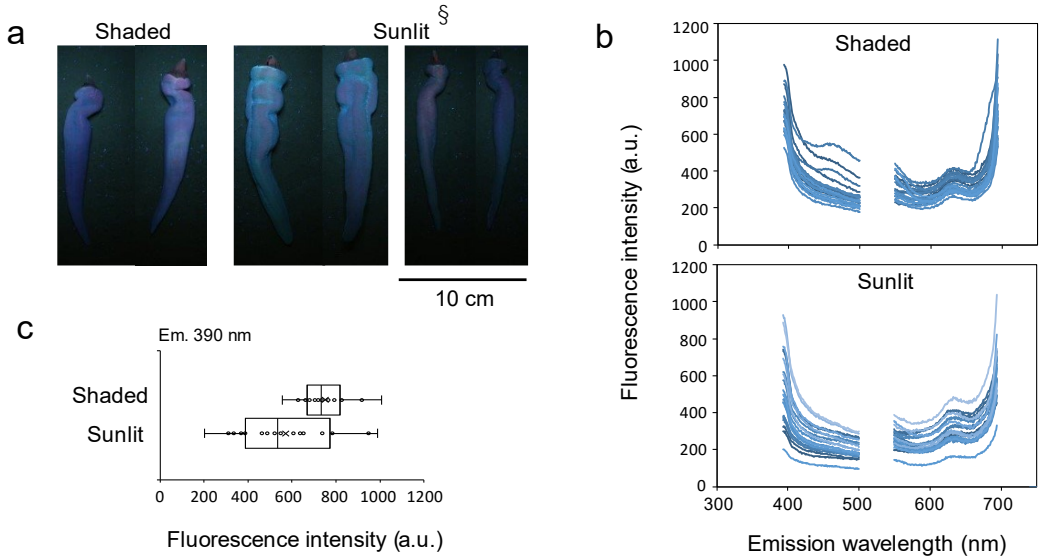

Fig. 1 (a) Fluorescence image of sweet pepper at 365 nm excitation. Two types of fluorescence patterns were observed under sunlit conditions. (b) Fluorescence spectrum at 360 nm excitation. (c) 390 nm fluorescence emission intensity (360 nm excitation). Two groups are shown: high (normal) and low (half of the normal) sunlight exposure. n = 20 for each group. Fluorescence intensities at ~550 nm and >695 nm were excluded (see the experimental section). (a) § Two patterns were observed for the sunlit conditions: bright- and dark-fluorescent sweet peppers. (b) No excitation light was observed above 390 nm. (c) The average values for the two conditions were significantly different ($P < 0.05$).

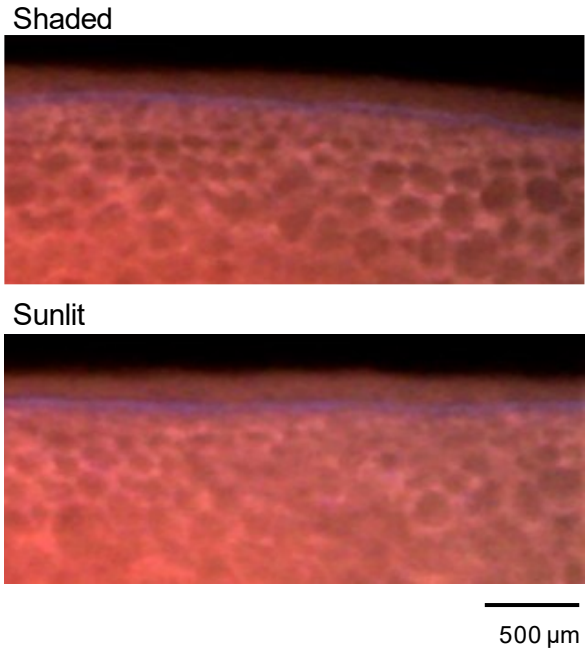

Fig. 2 Fluorescence microscopy images of the pericarp cross-section samples of sweet pepper at 365 nm excitation. Two groups are shown: high (normal) and low (half of the normal) sunlight exposure. The black-red interface in the upper region is the surface of the fruit.

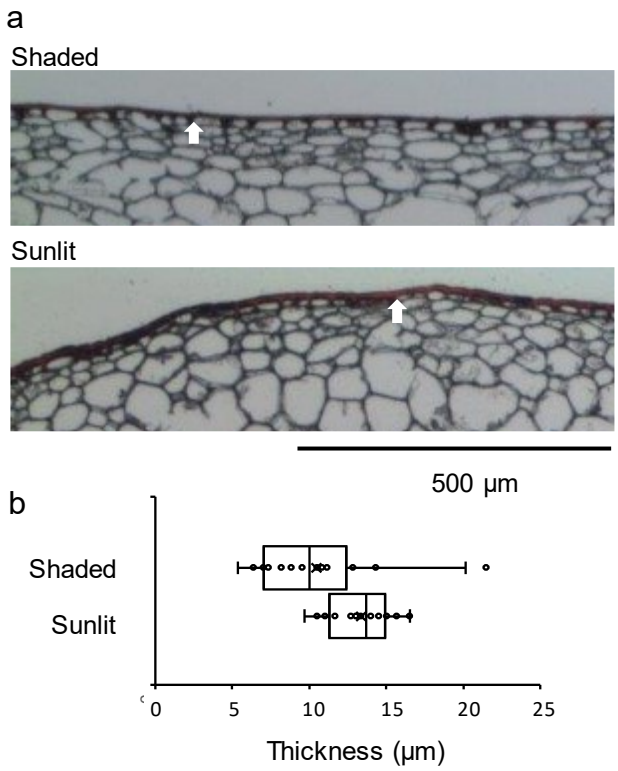

1 9

2 0 **Fig. 3** (a) Microscopic images of Oil Red O-stained cuticle. The cuticle is stained red (white arrows).

2 1 (b) Thickness of the epidermal cell wall. Two groups are shown: high (normal) and low (half of the

2 2 normal) sunlight exposure. n = 20 for each group. (b) The average values for the two conditions were

2 3 significantly different ($P < 0.05$).

2 4

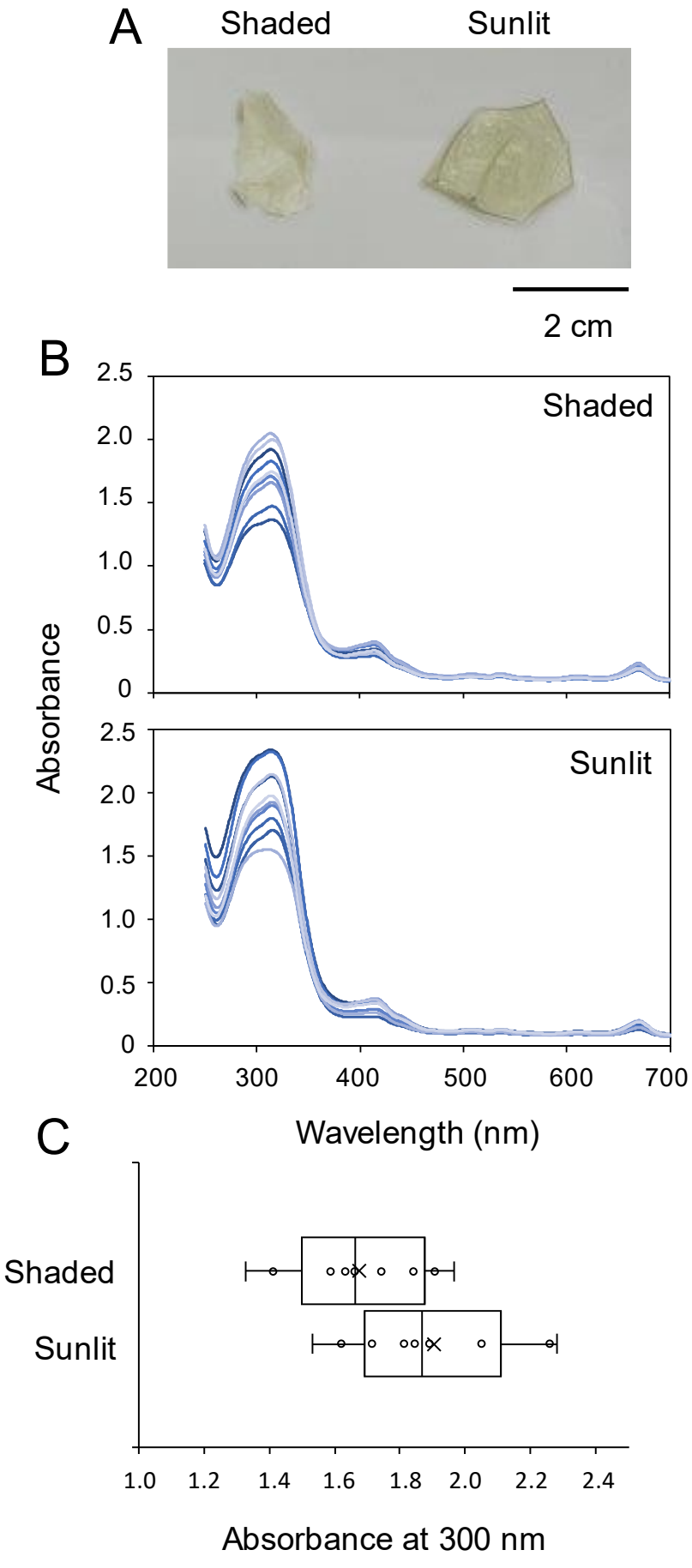
A
Shaded
Sunlit
2 cm
B
Shaded
Sunlit
Absorbance
2.5
2.0
1.5
1.0
0.5
0
200
300
400
500
600
700
Wavelength (nm)
C
Shaded
Sunlit
1.0
1.2
1.4
1.6
1.8
2.0
2.2
2.4
Absorbance at 300 nm

Fig. 4 (a) Photograph of the isolated epidermal cell wall of sweet pepper. (b) Diffuse transmission spectra of the epidermal cell wall. (c) Absorbance of the epidermal cell wall at 300 nm. Two groups are shown: high (normal) and low (half of the normal) sunlight exposure. n = 10 for each group. (c) The average values for the two conditions were significantly different ($P < 0.1$).

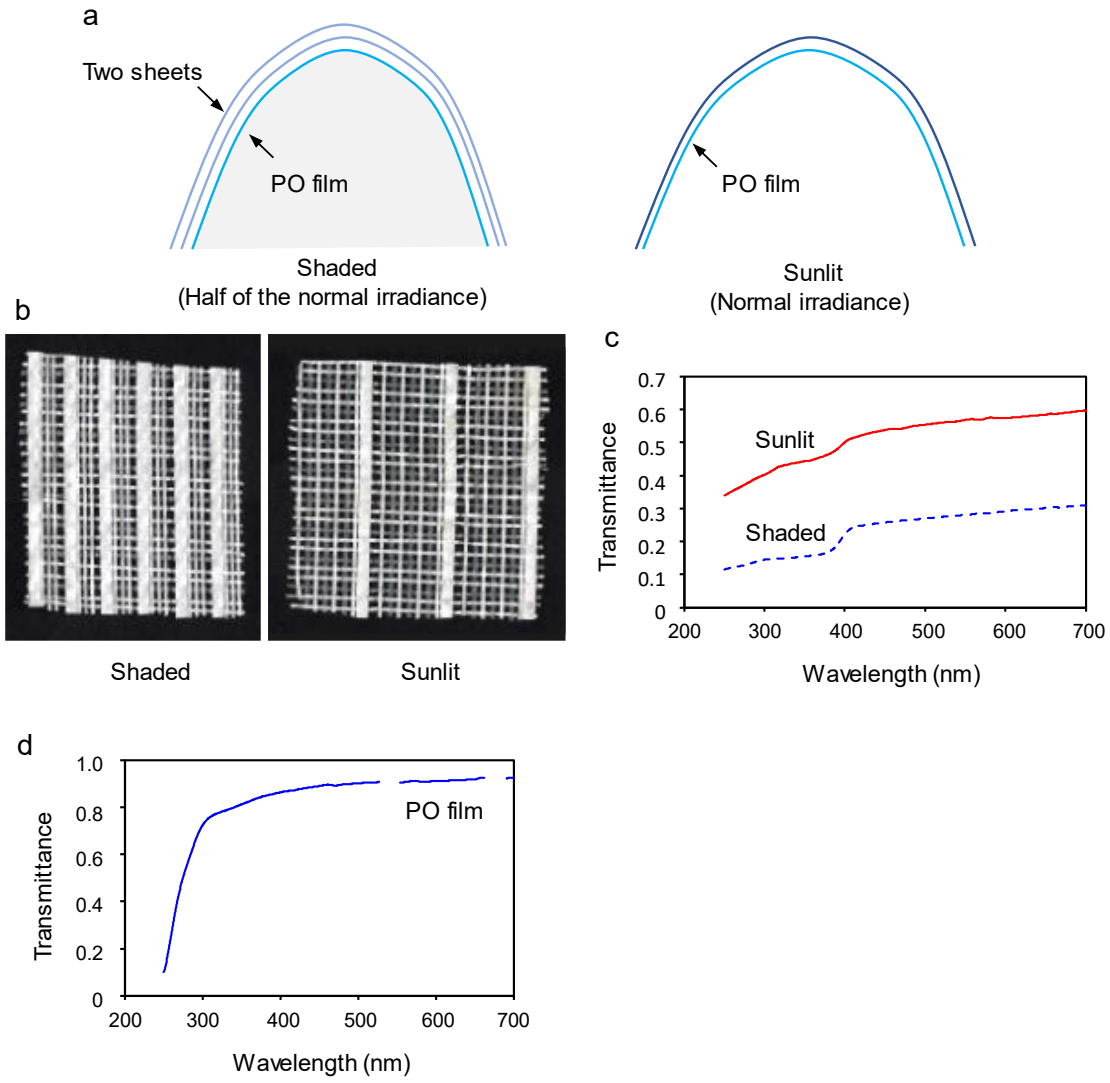

Fig. S1 (a) Schematic of a cultivation house with different solar exposures. (b) Photographs of the shading material. (c) Transmission spectra for each calculated cultivation condition (irradiance with polyolefin (PO) film is regarded as 1.0). (d) Transmission spectra of the polyolefin film. Spectral distortions were removed at 550 and 670 nm due to the device's stability.

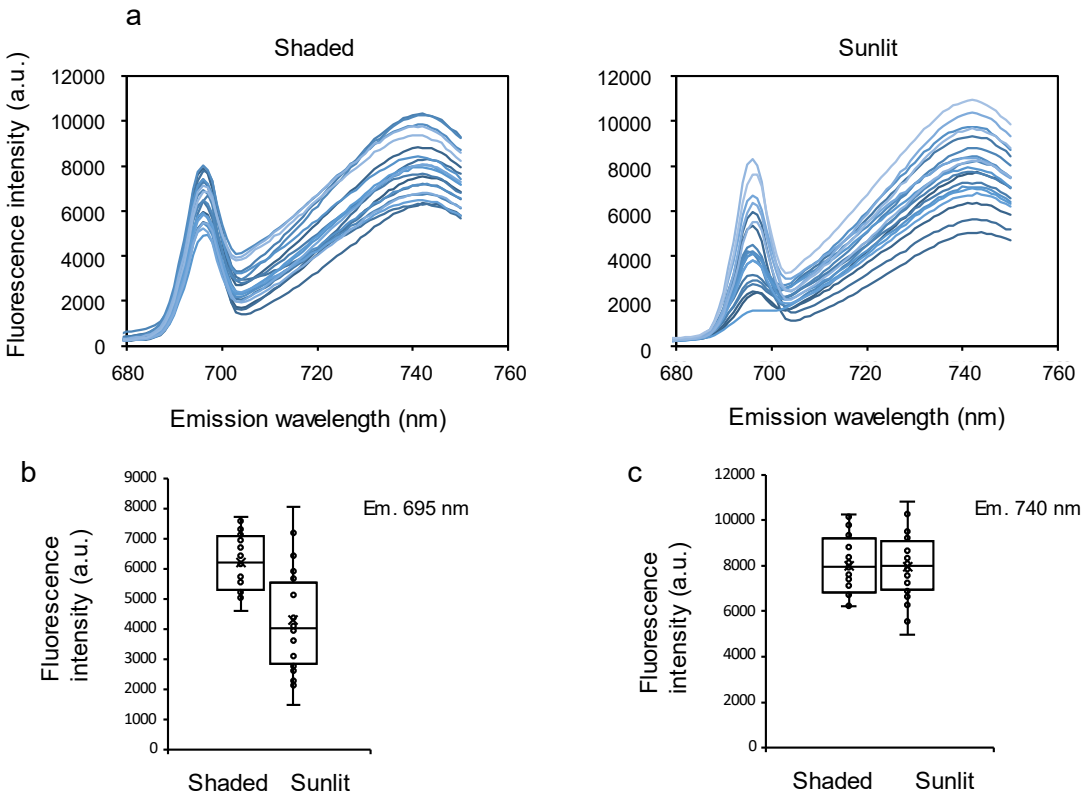

Fig. S2 (a) Red and near-infrared fluorescence spectra of sweet peppers at 460 nm excitation. (b) Red fluorescence intensity (695 nm emission) and (c) near-infrared fluorescence intensity (740 nm emission). Two groups are shown: high (normal) and low (half of the normal) solar exposure. Twenty samples were selected for each group. (b) The average values for the two conditions were significantly different ($P < 0.05$).

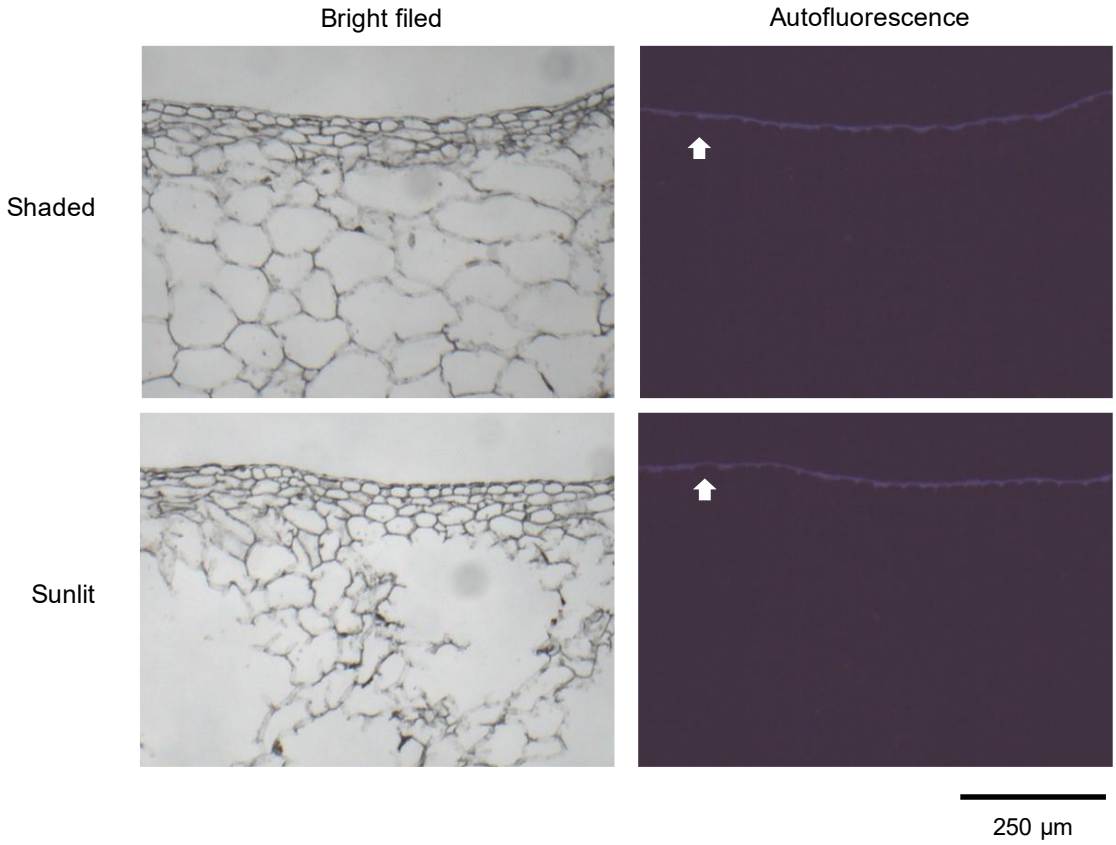

Fig. S3 Optical microscopic images (left, bright field) and autofluorescence microscopic images (right, 350 nm excitation) of the microtome sections of the pericarp. Low solar exposure (half of the normal) is shown in the upper row and high exposure (normal) is shown in the lower row. In the autofluorescence image, the epidermis emitted blue fluorescence (white arrow).

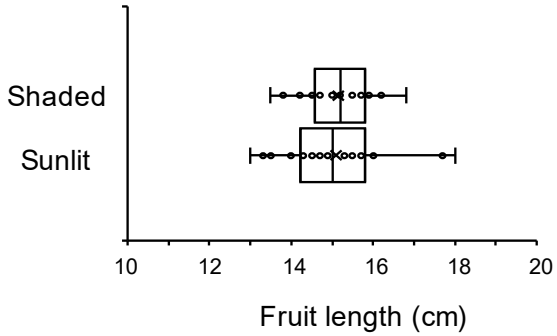

Fig. S4 Fruit length of sweet peppers. Two groups are shown: high (normal) and low (half of the normal) solar exposure. Twenty samples were selected for each group.

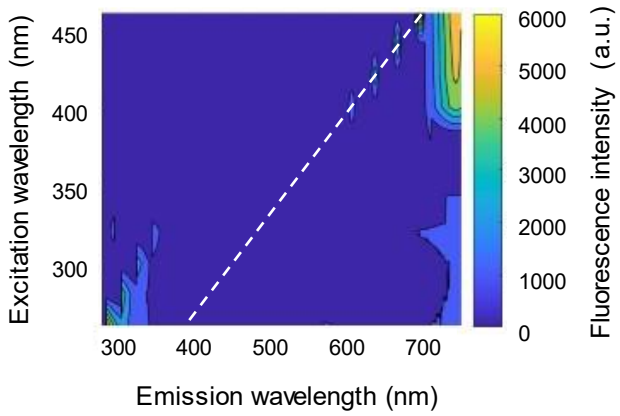

Fig. S5 An example of excitation–emission matrix of sweet pepper fruit pericarps. The white-dashed line, a linear-like wavelength function, indicates the Raman band (not fluorescence). At 360 nm excitation, the Raman band was observed near 550 nm and was excluded from the analysis (described in the experimental section). Strong red emission (a typical emission band of chlorophyll) was observed in the 400–460 nm excitation range.

Appendix

Estimation of mean spectral irradiance

In the main text, we discussed the integral irradiance based on shading material transmission and sweet pepper autofluorescent responses. However, we also expect that the the mean spectral irradiance were also beneficial to the readers, especially researchers on photon flux density [1], light quality [2], ultraviolet (UV) responses [3] and continuous wave responses [4]. Therefore, we present an example of data calculated by time, geographical coordinates and experimental parameters. In this section, we have also shown the estimation of spectral irradiance based on the Bird model [5] excel file provided by the National Renewable Energy Laboratory, United States Department of Energy [6].

1. Bird model

Spectral irradiance on the horizontal surface can be expressed as

$$I_T = I_d\cos(Z) + I_s. \quad \text{Eq. (A1)}$$

where I_T is the total irradiance (W m^{-2} or divided by μm when drawn as a function of the wavelength), I_d and I_s are the direct and diffuse components, respectively, and Z is the solar zenith angle. Alternatively, the direct radiation component (I_d) can be represented by the formula below.

$$I_d = H_0 D T_r T_a T_w T_o T_u.$$

Eq. (A2)

Here, H_0 is the extraterrestrial irradiance at the mean earth–sun distance. We also used the data revised by Neckel and Labs (1981) [7], originally presented by Fröhlich and Wehrli (1981), in this calculation. However, D is the correction factor for the earth–sun distance:

$$D = 1.00011 + 0.034221\cos\psi + 0.00128\sin\psi + 0.000719\cos2\psi + 0.000077\sin2\psi$$

Eq. (A3)

$$\psi = 2\pi(d - 1)/365$$

Eq. (A4)

where d is the day number within a year (1–365) and T_r, T_a, T_w, T_o and T_u are the atmospheric transmission parameters for Rayleigh scattering, aerosol attenuation (assumed as $10^{-0.005}$ in this study), water vapour absorption, ozone absorption and uniformly mixed gas absorption, respectively. For I second term in Eq. (A1), the diffuse or scattering component (I_s) can be expressed as shown below.

$$I_s = I_r + I_d + I_g.$$

Eq. (A5)

where I_r, I_d and I_g are the Rayleigh scattering component, aerosol scattering component and the component that accounts for multiple irradiance reflections between the ground and air, respectively.

2. Experimental parameters

In this calculation, we used some experimental parameters. For example, the day used that affects D in Eq. (A3) was 15 July 2021, representing the fruit elongation period from the fruit set (15 July) to the harvest (29 July). However, the geographic coordinate affecting the atmosphere's optical density was set as N 35.01°, E 135.56° (Kameoka, Kyoto, Japan). Additionally, the wavelength range was 0.3–0.7 μm. Besides, while the clear sky was modelled by summing I_d and I_s (= I_T), cloudy was modelled by only I_s.

3. Results

Fig. A1 shows the mean spectral irradiance from fruit set to harvest obtained by the Bird model and experimental parameters. Fig. A1a, b also depicts the irradiance as a function of time in a day. Regardless of the clear sky and cloudy days, the irradiance from 9:00 to 15:00 was around double that between 9:00 and 18:00. We also observed that the spectral shape suggested intense wavelength orders. Furthermore, while on a clear sky day, the irradiance of green was highest with a peak, followed by longer and shorter wavelengths (red and blue, and UV, respectively); the irradiance at the shorter wavelength was intense on a cloudy day due to the large contribution of shorter wavelength light to Rayleigh scattering and the diffuse component. Therefore, the irradiance was highest for green, followed by blue, UV and red (inversely).

Fig. A1c, d compares the two outdoor conditions in the greenhouse –normal irradiance (called sunlit) and half of the normal irradiance (called shaded). Investigations revealed that the irradiance for the inside condition was about half that of the outdoor condition. Within the greenhouse, the shaded condition was also approximately half of the sunlit condition. Moreover, the spectral irradiance was significantly attenuated in the UV region. This finding

was explainable by the low transmission of the polyolefin film and shading materials used (Fig. S1).

The mean photosynthetic photon flux density is also important for predicting crop yield (Table A1). Therefore, the photosynthetic photon flux density was obtained by converting the irradiance using photon molar energy after integrating the wavelength range of the photosynthetic active radiation (400–700 nm). Results showed that the photosynthetic irradiance for the clear sky day was 460 W m^{-2} (i.e., 2100 μmol m^{-2} s^{-1} for photon flux density), approaching the light saturation point of chilli peppers [8]. Meanwhile, the two experimental conditions–sunlit and shaded–were approximately half and quarters of the light saturation point, respectively. For the cloudy sky, the irradiance was estimated approximately one-tenth of those at the clear sky.

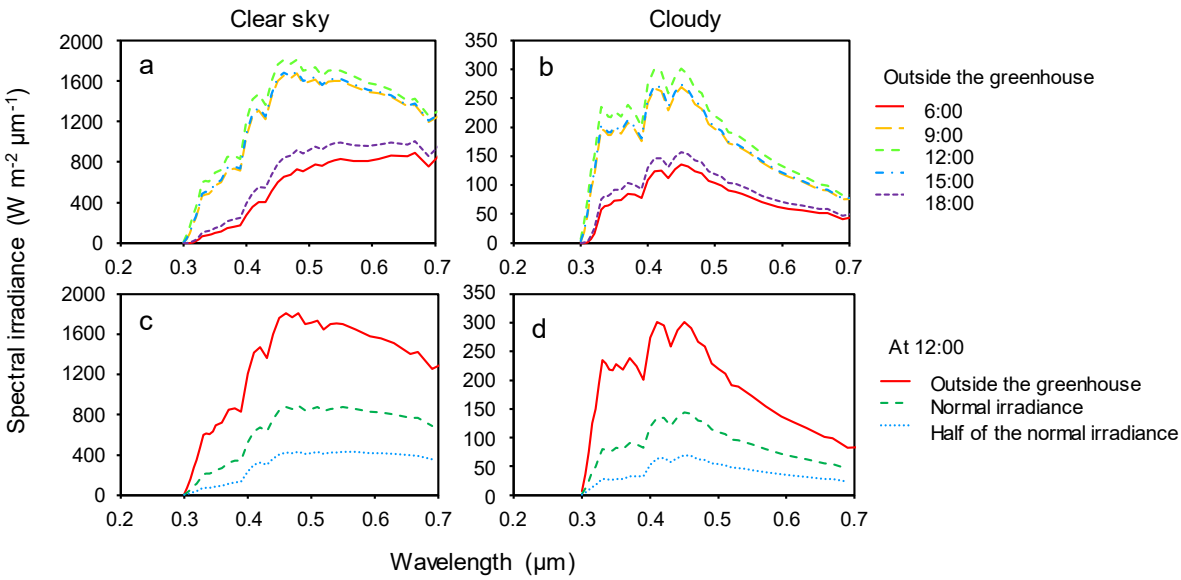

Fig. A1 Spectral irradiance as a function of time and geographic coordinates. The spectral irradiance, as of 15 July 2021, at Kameoka, Kyoto, Japan (N 35.01°, E 135.56°), was calculated by the Bird model [5] and the measured transmission of the polyolefin film and shading materials. The calculation programme is available online under the permission of the National Renewable Energy Laboratory, United States Department of Energy [6]. (a, b) Spectral irradiance at 9, 12, 15 and 18:00. (a) Clear sky and (b) cloudy days. (c, d) Spectral irradiance at noon for outside, sunlit and shaded greenhouse conditions. (c) Clear sky and (d) cloudy days.

Table A1 Photosynthetic irradiance and photon flux density

	Clear sky‡			Cloudy‡		
	Outdoors	Indoors		Outdoors	Indoors	
		Sunlit	Shaded		Normal	Shaded
Irradiance† (W m^{-2})	460	230	110	56	28	14
Photon flux density† (μmol m^{-2} s^{-1})	2100	1100	540	230	120	59

† Integral photosynthetic active radiation (0.4–0.7 μm) for both unit representations.

‡ Calculations based on the earth–sun mean distance as of 15 July 2021. The solar zenith angle at noon was calculated.

References

1. Sui, X., Mao, S., Wang, L., Zhang, B., & Zhang, Z. (2012). Effect of Low Light on the Characteristics of Photosynthesis and Chlorophyll a Fluorescence During Leaf Development of Sweet Pepper. *Journal of Integrative Agriculture*, *11*(10), 1633–1643. https://doi.org/10.1016/S2095-3119(12)60166-X
2. Diel, M. I., Valera, O. V. S., Pinheiro, M. V. M., Thiesen, A., Meira, D., de Melo, P. J., Junges, D. L., Otomar, B., & Schmidt, D. (2019). Temperature and light quality influence seed germination of two biquinho pepper cultivars. *Bulgarian Journal of Agricultural Science*, *25*(5), 1007–1014.
3. Rodríguez-Calzada, T., Qian, M., Strid, Å., Neugart, S., Schreiner, M., Torres-Pacheco, I., & Guevara-González, R. G. (2019). Effect of UV-B radiation on morphology, phenolic compound production, gene expression, and subsequent drought stress responses in chili pepper (*Capsicum annuum* L.). *Plant Physiology and Biochemistry*, *134*, 94–102. https://doi.org/10.1016/j.plaphy.2018.06.025
4. Joshi, N. C., Ratner, K., Eidelman, O., Bednarczyk, D., Zur, N., Many, Y., Shahak, Y., Aviv-Sharon, E., Achiam, M., Gilad, Z., & Charuvi, D. (2019). Effects of daytime intra-canopy LED illumination on photosynthesis and productivity of bell pepper grown in protected cultivation. *Scientia Horticulturae*, *250*, 81–88. https://doi.org/10.1016/j.scienta.2019.02.039
5. Bird, R. E., & Riordan, C. (1986). Simple Solar Spectral Model for Direct and Diffuse Irradiance on Horizontal and Tilted Planes at the Earth's Surface for Cloudless Atmospheres. *Journal of Applied Meteorology and Climatology*, *25*(1), 87–97. https://doi.org/10.1175/1520-0450(1986)025<0087:SSSMFD>2.0.CO;2
6. NREL. (2022). *Bird Simple Spectral Model | Grid Modernization*. https://www.nrel.gov/grid/solar-resource/spectral.html
7. Neckel, H., & Labs, D. (1981). Improved Data of Solar Spectral Irradiance from 0.33 to

1.25 μ. *Physics of Solar Variations, Proceedings of the 14th ESLAB Symposium Held in Scheveningen, The Netherlands, 16–19 September, 1980*, 231–249. https://doi.org/10.1007/978-94-010-9633-1_27

8. Masabni, J., Sun, Y., Niu, G., & Valle, P. D. (2016). Shade Effect on Growth and Productivity of Tomato and Chili Pepper. *HortTechnology*, *26*(3), 344–350. https://doi.org/10.21273/HORTTECH.26.3.344